SALT-FINGER CONVECTION IN A STRATIFIED FLUID LAYER INDUCED BY THERMAL AND SOLUTAL CAPILLARY MOTION

C. F. Chen and Cho Lik Chan

Department of Aerospace and Mechanical Engineering
The University of Arizona
Tucson, AZ 85721

ABSTRACT

Salt-finger convection in a double-diffusive system is a motion driven by the release of gravitational potential due to differential diffusion rates. The normal expectation is that, when the gravitational field is reduced, salt-finger convection together with other convective motions driven by buoyancy forces will be rapidly suppressed. However, because the destabilizing effect of the concentration gradient is amplified by the Lewis number, with values varying from 10^2 for aqueous salt solutions to 10^4 for liquid metals, salt-finger convection may be generated at much reduced gravity levels. In the microgravity environment, the surface tension gradient assumes a dominant role in causing fluid motion. In this paper, we report some experimental results showing the generation of salt-finger convection due to capillary motion on the surface of a stratified fluid layer. A numerical simulation is presented to show the cause of salt-finger convection.

INTRODUCTION

When a fluid contains two diffusing components with different molecular diffusivities, convective motion may be generated when potential energy is released owing to differential diffusion. In the case of a warm and solute-rich fluid overlying cold and fresher fluid with an overall density distribution that is gravitationally stable, convection will be generated through the finger instability mechanism of the double-diffusive system. The critical condition is given by Stern (ref. 1) for a free-free layer:

$$R_s \text{Le} = R_T + \frac{27\pi^4}{4} \tag{1}$$

in which the solute and thermal Rayleigh numbers are defined as

$$R_S = \frac{g\alpha_s \Delta S d^3}{\kappa\nu} \quad , \quad R_T = \frac{g\alpha\Delta T d^3}{\kappa\nu} \tag{2}$$

with g the gravitational acceleration; α_s and α the volumetric expansion coefficients due to the solute and temperature, respectively; ΔS and ΔT the changes in solute and temperature across the fluid layer with thickness d; κ the thermal diffusivity; and ν the kinematic viscosity. The Lewis number, defined as $\text{Le} = \kappa/\kappa_s$, where κ_s is the mass diffusivity, is generally quite large, being $\sim 10^2$ for aqueous salt solutions and $\sim 10^4$ for liquid metals. The constant $27\pi^4/4$ is for free-free boundary conditions only. For other conditions, it is of order 10^3.

In laboratory experiments and in practice, the convecting cells are long and narrow (aptly named fingers), with upward and downward flow in alternating cells. Because of the large magnitudes of Le, the critical condition for the onset of finger convection can be exceeded under reduced gravity levels. Using the thermophysical properties for a lead-tin alloy as given by Coriell et al. (ref. 2) and letting $g = \varepsilon g_0$, where g_0 is the sea-level gravity, the critical condition for the onset of finger convection becomes

$$\varepsilon\Delta S d^3 > \frac{10^3 \kappa_S \nu}{g_0 \alpha_S} = 1.43 \times 10^{-5} \text{ wt\%-cm}^3 \tag{3}$$

in which ΔS is in wt%. For $d = 1$ cm and $\Delta S = 1$ wt%, $\varepsilon = 10^{-5}$, or finger convection may be triggered at $10^{-5} g_0$. We note here that the thermal Rayleigh number at this gravity level is

$$R = 0.438 \times 10^3 \varepsilon \Delta T = 0.4 \times 10^{-2} \Delta T \tag{4}$$

which is negligible compared to LeR_S for reasonable values of ΔT. For an ethanol-water solution with 98% ethanol, finger convection may occur at $10^{-4} g_0$ for a comparable layer thickness and concentration difference. Under microgravity conditions, thermocapillary flow is easily generated. If this motion occurs on the surface of a stratified fluid layer, might not finger convection be caused to onset? We have made experimental investigations into this possibility and found the answer to be affirmative. Numerical simulations indicate that the thermocapillary effect is the main cause of this phenomenon.

In order to minimize the effect of buoyancy-driven convection, the experiment was conducted in a stratified ethanol-water solution with pure ethanol on the surface. A small ΔT was imposed across the tank to generate the thermocapillary flow. It is known that when the ΔT exceeds the critical value, a vertical array of nearly horizontal convection cells are generated. This problem of sideways heating of a solute gradient has been investigated experimentally by Thorpe et al., Chen et al., Tanny and Tsinober, and Lee et al. (refs. 3-6). Numerical simulations of this problem have been made by Wirtz et al. (ref. 7), Heinrich (ref. 8), and, more recently, by Lee and Hyun (ref. 9). In the experiments we conducted, the ΔT was limited to 1°C or 2°C, well below the critical value of 6°C, and the fluid in the rest of the tank remained motionless, except in the layer near the bottom boundary where convection was induced by the end conditions.

EXPERIMENTAL APPARATUS AND PROCEDURE

Experiments were carried out in a tank 5 cm wide × 10 cm high × 9.5 cm long. The two sidewalls (10 cm × 9.5 cm) are made of chrome-plated copper, with passages provided for circulating fluid from two constant-temperature baths. The two end walls are made of plexiglass, and the bottom of Bakelite. A thermocouple was mounted on a vertical transverse mechanism located at the center of the tank to measure the temperature distribution of the fluid. The fluid used was an ethanol-water solution; it was chosen because its free surface is not easily contaminated. The concentration varied from 100 wt% ($\rho = 0.791 \text{ g cm}^{-3}$) at the top to 64 wt% ($\rho = 0.883 \text{ g cm}^{-3}$) at the bottom. This relatively large stable density gradient was chosen so that the critical ΔT for the onset of horizontal cellular convection would not be exceeded during our experiments. This value of ΔT_c is 6.4°C according to the stability analysis carried out by Thorpe et al. (ref. 3). In our experiments, the ΔT was obtained by increasing (decreasing) the temperature of the hot (cold) wall by $\Delta T/2$.

Flow visualization was carried out either by shadowgraph or by particle trace. For the latter, aluminum powder was added to the fluid. A 20-mW He-Ne laser with a cylindrical lens was used to provide a horizontal sheet of light through the tank. A CCD video camera was mounted vertically above the tank, and the image of the particle motion was viewed on a monitor and simultaneously recorded by a time-lapse VCR. The test tank was mounted on a platform capable of vertical motion. In this manner, particle traces could be viewed at any horizontal plane within the 10-cm height of the test tank.

Twenty-one layers, each containing 21.5 cm³ of solutions of decreasing density, were successively introduced into the tank to obtain the initial stratification. For the ethanol-water solution, the diffusivity varied nonlinearly with the concentration from $0.41 \times 10^{-5} \text{ cm}^2/\text{s}$ at 64% ethanol to $1.15 \times 10^{-5} \text{ cm}^2/\text{s}$ at 100% ethanol. Since we have no means of measuring the concentration of ethanol, the diffusion process was simulated by a one-dimensional calculation taking into account the effect of variable diffusivity. The concentration distribution at 1 hr after the start of the diffusion process was essentially linear with height, with nondiffusive effects near the top and bottom. With these results in mind, the test procedure followed was to begin all experiments 1 hr after completion

of the filling process. For flow visualization tests, aluminum particles were added to the prepared solutions for each layer prior to filling the tank.

RESULTS AND DISCUSSION

Experiments were conducted with a free and a rigid top boundary. For the free-surface experiment, salt-finger convection was induced soon after the ΔT was imposed. (These are illustrated in a series of four particle-trace photographs taken from the video display with an 8-sec exposure.) During this experiment, the first ΔT step of 0.8°C was imposed at 10:10. Particles at a level 0.5 cm below the free surface were seen to move slowly from the hot wall toward the cold wall soon after the ΔT was imposed. Fig. 1a shows a particle trace photograph taken at 10:14. Motion of the particles can be discerned, but there were no apparent salt fingers. At 10:18, Fig. 1b, finger convection was clearly exhibited. It is noted here that finger convection in the presence of shear, which is present in our experiments, appears in longitudinal sheets aligned with the direction of shear. This phenomenon, similar to the case of Rayleigh-Benard convection in the presence of shear, was clearly shown by Linden (ref. 10) in counterflowing streams of sugar and salt solutions. The onset of salt fingers near the cold rather than the hot wall is due to the large effect of solute concentration on surface tension, and this point is further discussed in the section on numerical simulation. By 10:32, Fig. 1c, fingers reached across approximately 3/4 of the width of the tank, and the transverse velocity became less, due to the smaller temperature gradient. At 11:20, the ΔT was increased to 1.9°C and, at 11:55, Fig. 1d, the fingers were quite well organized across the entire width of the tank. In experiments conducted with the rigid top boundary, no finger convection was observed at comparable ΔT's.

The observed difference between the free-surface and the rigid-surface experiments can be explained in terms of the temperature and density distributions. Since there is no easy method of measuring the concentration of ethanol in situ, we infer its distribution from the measured temperature distribution by comparing the results obtained in our earlier experiments with salt solution in which concentration and temperature were simultaneously measured. In the present experiments, temperature was measured along the vertical centerline of the tank at 2.5 mm intervals. The results for the free-surface case and the rigid-surface case are shown in Fig. 2. In both cases, the temperature distributions at $\Delta T = 1°C$, 2°C, and 3°C are shown. For the free-surface case, it is seen that, at $\Delta T = 1°C$, temperatures in the top 1 cm are slightly higher than the rest of the fluid because of the motion at the surface due to the surface tension gradient. The temperature difference between the surface and the rest of the fluid became larger as ΔT was increased. One also notes that there was a layer of fluid at the top, 2-4 mm in thickness, in which the temperature was constant, indicating that the fluid was well mixed due to finger convection. The results for the rigid surface show a small, positive temperature gradient near the top. The characteristics of temperature distribution at $\Delta T = 2°C$ were quite similar to the data obtained at $\Delta T = 2.1°C$ with the salt solution, in which the concentration measurement at the same time indicated a stable gradient essentially unchanged from the initial distribution. In fact, this stable concentration gradient persisted to $\Delta T = 3.8°C$. From these results, we infer that, in the comparable experiment with a rigid top surface at ΔT up to 2°C, the initial stable ethanol gradient still persisted and the fluid was motionless. At $\Delta T = 3°C$, the temperature distribution indicates there was motion but, because of the stable concentration and temperature gradients, no fingers were observed.

NUMERICAL SIMULATION

Numerical simulation using a transient two-dimensional finite difference method (FDM) was performed. The geometry simulated is a 1 × 5 rectangular domain. The fluid is initially at uniform temperature, with stably stratified ethanol-water solution. The initial concentration distribution is essentially linear, with nondiffusive effects near the top and bottom. At time zero, nondimensional temperatures at the left and right sidewalls are set and maintained at 0.5 and -0.5, respectively. The relevant dimensionless parameters are $R_T = 100$, $R_S = 1000$, $M_T = 8000$, $M_S = 40,000$, $Pr = 17$, and $Le = 85$. These correspond to $\Delta T = 1°C$, $\Delta S = 4$ wt%, and a 1-cm height scale. The gravitational field is $10^{-3} g_0$. The two-dimensional simulation clearly captured the mechanism that led to salt fingers.

The imposed temperature conditions at the sidewalls established very strong temperature gradients near the upper corners, as shown in Fig. 3a. Consequently, two counter-clockwise vortices are established due to thermocapillarity. These vortices bring high-concentration solution to the free surface, creating a nonuniform concentration on the free surface, as shown in Fig. 3b. Near the hot wall (left), the concentration on the free surface

321

produces a surface tension force opposing the thermocapillarity. However, the concentration on the free surface near the cold wall (right) reinforces the thermocapillarity. This can be seen clearly in Fig. 3c, where the total surface tension effect $[(M_S/M_T)S - T]$ is plotted. Consequently, the vortex near the hot wall decays while the vortex near the cold wall grows, which greatly distorts the temperature and concentration fields. The vertical temperature distribution near the cold wall ($x = 4.75$), as shown in Fig. 4a, is stabilizing. The vertical concentration distribution, shown in Fig. 4b, is initially stably stratified. However, at later times, the rotation brings high-concentration solution to the top, creating a destabilizing effect. Based on the temperature and concentration distributions and the corresponding length scale, we estimated that $R_S = 167$ and $R_T = 15$. According to Eq. (1), this is in the supercritical regime for salt-finger instability. The total vertical density $[(R_S/R_T)S - T]$ distribution is plotted in Fig. 4c. The top-heavy situation can be seen clearly. This unstable situation is responsible for the onset of salt fingers near the cold wall and their propagation throughout the tank as observed in our experiments.

CONCLUSIONS

When a fluid layer is stratified by a solute concentration and has a top free surface, thermocapillary motion is generated as soon as a small ΔT across the tank is imposed. Due to the initial density stratification, no motion is induced in the rest of the fluid at this small ΔT. The capillary motion near the cold wall brings the warmer and solute-rich fluid to the surface and causes the onset of finger convection. This is an effective means of generating finger convection in a microgravity environment. Since the conditions at onset are likely to be in the neighborhood of the critical state, finger convection would appear in rolls, with lateral dimensions comparable to the layer thickness.

ACKNOWLEDGMENT

REFERENCES

1. Stern, M. E., "The 'Salt-Fountain' and Thermohaline Convection," *Tellus*, Vol.12, pp. 172-175, 1960.

2. Coriell, S. R., Cordes, M. R., and Boettinger, W. J., "Convective and Interfacial Instabilities During Unidirectional Solidification of a Binary Alloy," *J. Crystal Growth*, Vol. 49, pp. 13-28, 1980.

3. Thorpe, S. A., Hutt, P. K., and Soulsby, R., "The Effects of Horizontal Gradients on Thermohaline Convection," *J. Fluid Mech.*, Vol. 38, pp. 375-400, 1969.

4. Chen, C. F., Briggs, D. G., and Wirtz, R. A., "Stability of Thermal Convection in a Salinity Gradient Due to Lateral Heating," *Int. J. Heat Mass Transfer*, Vol. 14, pp. 57-65, 1971.

5. Tanny, J. and Tsinober, A. B., "The Dynamics and Structure of Double-Diffusive Layers in Sidewall Heating Experiments," *J. Fluid Mech.*, Vol. 196, pp. 135-156, 1988.

6. Lee, J., Hyun, M. T., and Kang, Y. S., "Confined Natural Convection Due to Lateral Heating in a Stably Stratified Solution," *Int. J. Heat Mass Transfer*, Vol. 33, pp. 869-875, 1990.

7. Wirtz, R. A., Briggs, D. G., and Chen, C. F., "Physical and Numerical Experiments on Layered Convection in a Density-Stratified Fluid," *Geophys. Fluid Dyn.*, Vol. 3, pp. 265-288, 1972.

8. Heinrich, J. C., "A Finite Element Model for Double-Diffusive Convection," *Int. J. Num. Meth. Eng.*, Vol. 20, pp. 447-464, 1984.

9. Lee, J. W. and Hyun, M. T., "Time-Dependent Double Diffusion in a Stably Stratified Fluid Under Lateral Heating," *Int. J. Mass Heat Transfer*, Vol. 34, pp. 2409-2415, 1991.

10. Linden, P. F., "Salt Fingers in a Steady Shear Flow," *Geophys. Fluid Dyn.*, Vol. 6, pp. 1-27, 1974.
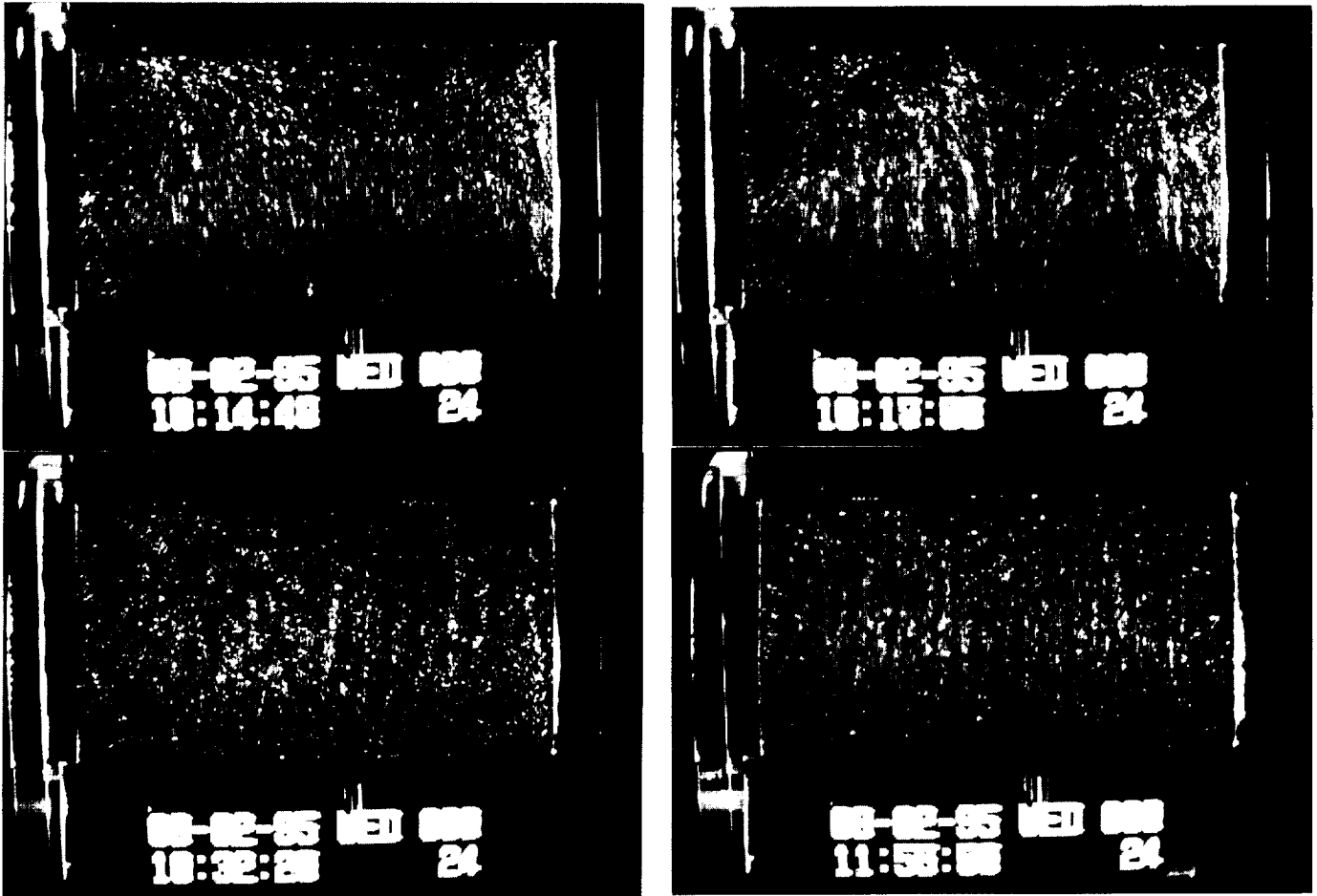
Fig. 1. Particle trace at 0.5 cm below the free surface, 8-sec exposure. Cold wall at bottom. Experiment started with $\Delta T = 0.8°C$ at $t = 10:10$. Δt increased to $1.9°C$ at $t = 11:20$.
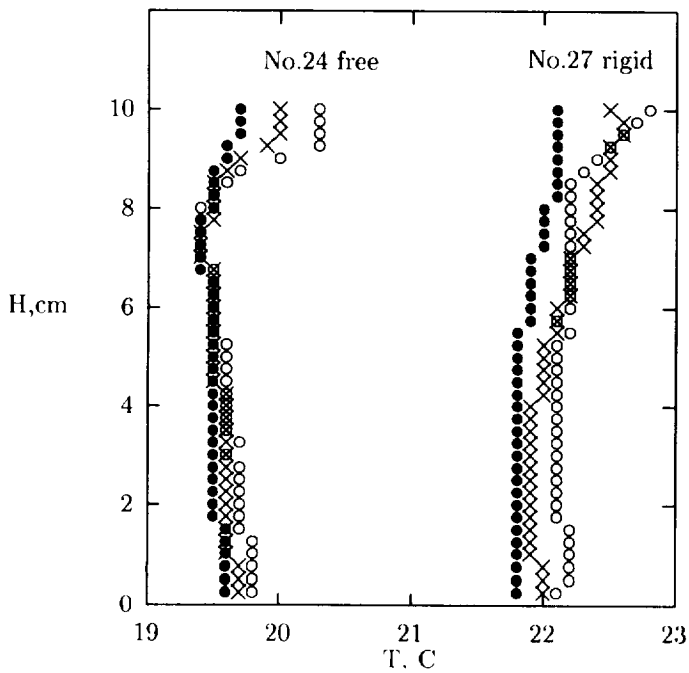

Fig. 2. Vertical temperature distribution for the free and rigid top surfaces.

- $\Delta T = 1°C$
- × $\Delta T = 2°C$
- ○ $\Delta T = 3°C$
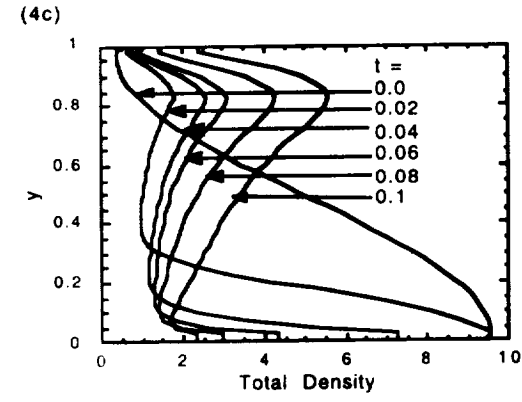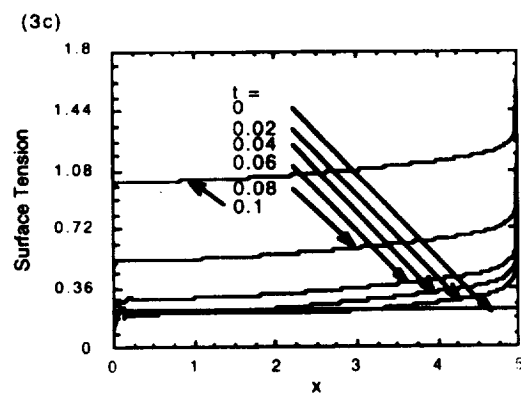
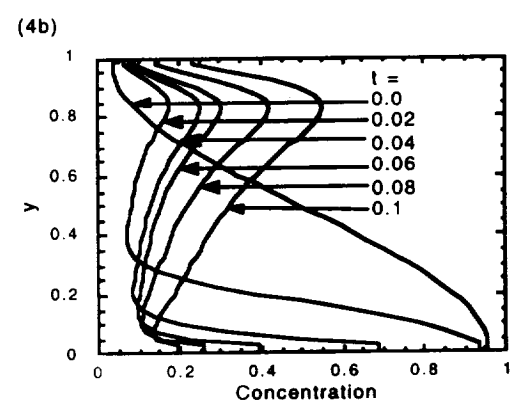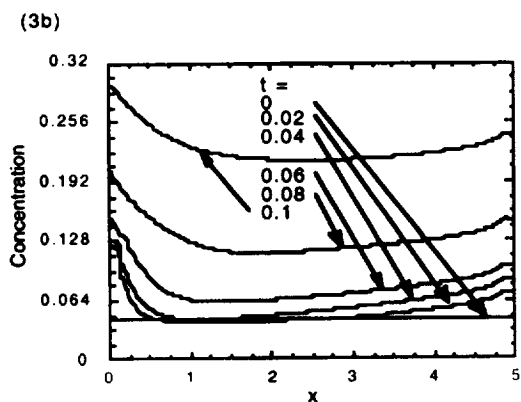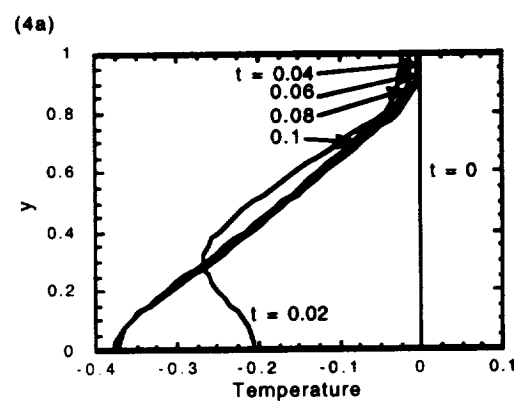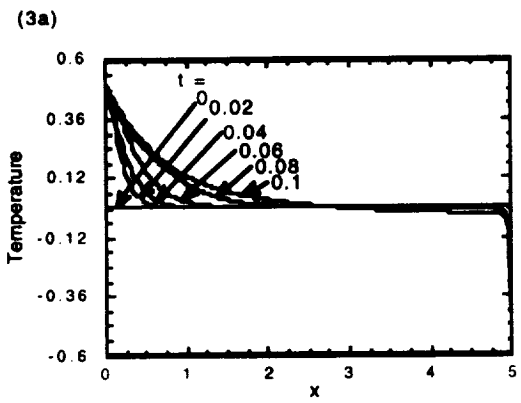Fig. 3. Temperature, concentration, and surface tension distributions on the free surface.

Fig. 4. Temperature, concentration, and total density distributions (vertical) near the cold wall (x = 4.75).

324